AD-785 579

DEVELOPMRNT OF AN IMPROVED DESIGN TOOL FOR PREDICTING AND SIMULATING HELICOPTER ROTOR NOISE

H. Kevin Johnson

Rochester Applied Science Associates, Incorporated

Prepared for:

Army Air Mobility Research and Development Laboratory

June 1974

EUSTIS DIRECTORATE POSITION STATEMENT

The report has been reviewed by the Eustis Directorate, U. S. Army Air Mobility Research and Development Laboratory and is considered to be technically sound.

The information presented is an extension of research performed earlier concerning the prediction and simulation of noise generated by helicopter rotors. The new effort has enhanced the earlier results by accounting for the effects of ground reflection, blade passage variability, and blade/vortex interaction on the helicopter rotor noise as perceived by an observer.

A computer program capable of predicting a particular helicopter's noise signature was the product of this research effort. This program is documented at the Eustis Directorate, U. S. Army Air Mobility Research and Development Laboratory and is available upon request for those interested in investigating helicopter rotor noise generation, prediction, and simulation.

The technical monitor for this contract was Mr. William T. Alexander, Jr., Technology Applications Division.

iii

Unclassified

REPORT DOCUMENTATION PAGE		READ INSTRUCTIONS BEFORE COMPLETING FORM
1. REPORT NUMBER USAAMRDL-TR-74-37	2. GOVT ACCESSION NO.	3. RECIPIENT'S CATALOG NUMBER AD-785 579
4. TITLE *(and Subtitle)* DEVELOPMENT OF AN IMPROVED DESIGN TOOL FOR PREDICTING AND SIMULATING HELICOPTER ROTOR NOISE		5. TYPE OF REPORT & PERIOD COVERED Final report
		6. PERFORMING ORG. REPORT NUMBER RASA Report 74-02
7. AUTHOR(*s*) H. Kevin Johnson		8. CONTRACT OR GRANT NUMBER(*s*) Contract DAAJ02-73-C-0061
9. PERFORMING ORGANIZATION NAME AND ADDRESS Rochester Applied Science Associates,Inc Rochester, New York		10. PROGRAM ELEMENT, PROJECT, TASK AREA & WORK UNIT NUMBERS Project 1F162204AA43
11. CONTROLLING OFFICE NAME AND ADDRESS Eustis Directorate U. S. Army Air Mobility R&D Lab Fort Eustis, Virginia 23604		12. REPORT DATE June 1974
		13. NUMBER OF PAGES 48
14. MONITORING AGENCY NAME & ADDRESS(*if different from Controlling Office*)		15. SECURITY CLASS. *(of this report)* Unclassified
		15a. DECLASSIFICATION/DOWNGRADING SCHEDULE

16. DISTRIBUTION STATEMENT *(of this Report)*

Approved for public release; distribution unlimited.

17. DISTRIBUTION STATEMENT *(of the abstract entered in Block 20, if different from Report)*

18. SUPPLEMENTARY NOTES

19. KEY WORDS *(Continue on reverse side if necessary and identify by block number)*

Helicopters
Noise (Sound)
Rotors

20. ABSTRACT *(Continue on reverse side if necessary and identify by block number)*

The helicopter rotor noise prediction program developed under Contract DAAJ02-71-C-0064 has been improved by the following four items: (1) inclusion of the helicopter rotor noise ground reflection phenomenon, (2) inclusion of the variability of oscillatory forces as related to the vortex shedding phenomenon, (3) expansion of the data base for the broadband noise data bank, and (4) description of a calculation procedure

DD _{1 JAN 73} FORM 1473   EDITION OF 1 NOV 65 IS OBSOLETE

Unclassified

20. Continued.

which demonstrates how the program input deck can be modified
to account for impulse signals of single-rotor blade vortex in-
teractions.

The rotor noise prediction program has been developed so that
the acoustic characteristics of new, untested rotor designs
could be evaluated as well as the effects of basic design
changes on the acoustic signature of existing rotors. The pre-
diction program is general enough to be able to consider future
designs in hover and steady-state flight for any observer
location. The program output can be Fourier analyzed so that
the noise spectrum can be generated. The digital pressure time
history can also be converted to an analog signal for subjec-
tive evaluation.

PREFACE

TABLE OF CONTENTS

LIST OF ILLUSTRATIONS

Figure

INTRODUCTION

Rotor noise is the primary contributor to the external noise of modern gas-turbine-powered helicopters. Results of several research programs (References 1,2, and 3) have shown that the acoustic pressure time history at an observer's location is due almost entirely to the noise output of the main and tail rotor systems. This means that the helicopter's detectability and to a large extent its effectiveness as a weapons system are determined by the noise signature of its rotor system.

It had been desired for many years to have some means of accurately predicting the detailed noise characteristics of a given rotor system during the design stage. If this were realizable, design studies could be carried out and tradeoffs between noise and performance clearly delineated. Further, for a rotor system designed to meet given performance requirements, the optimum acoustic design could be determined. It is believed that the key to the optimum design of a rotor as regards noise is a thorough understanding of the noise generating mechanisms so that noise reduction methods can be evaluated without undertaking an experimental program of rotor design and test. Several studies (References 1, 2, and 3) have concentrated on the aerodynamic mechanisms of rotor noise. The reports of these studies have shown the important aerodynamic mechanisms of noise generation for helicopter rotors. In order to use these results, however, an acoustic prediction program had to be devised that would allow subjective as well as scientific evaluation of helicopter rotor noise during the design stage.

There have been efforts to provide such a prediction method in the past. Attempts were first made by empirical relations and scaling to forecast the overall noise level for a rotor design. Following this, empirical approaches have been tried that will foretell the octave-band noise signature. But even if overall and octave-band forecast techniques are entirely accurate, they reveal extremely limited information about a rotor system which is yet to be built.

What is required is an analytical tool that can be applied to a given rotor system including main and tail rotors, or a tandem configuration, and that will provide for either hover or forward flight:

1. A plot of the predicted acoustic pressure time history for any observer's location relative to the aircraft.

1

2. A plot of the predicted SPL or spectrum.

3. A tape recording of the predicted rotor noise that can be played for subjective evaluation.

The advantages of such a tool are many. As noted, it can be used for rotor design in which an acoustic evaluation can be made of the effects of blade chord, airfoil section, twist, planform, and rotational speed. Rotor parameters such as solidity, thrust and number of blades could also be varied and the resulting noise signatures studied. Such a predictive tool would be of great value to both the manufacturers of helicopters and the users. To provide such a predictive method was the object of the program undertaken in Contract DAAJ02-71-C-0064 and reported in Reference 4. The effort reported herein is an extension of that work (Reference 4) so that the important effects of rotor noise ground reflection and rotor noise variability as related to oscillatory aero-dynamic forces associated with broadband noise are included in the predicted noise.

IMPROVEMENT OF THE NOISE PREDICTION PROGRAM

The helicopter rotor noise prediction program developed previously (Reference 4) has been expanded to include the following items which are important to the evaluation of the noise produced by rotors: (1) the ground reflection phenomenon, (2) the variability of oscillatory forces as related to the vortex shedding phenomena, (3) an expanded data base for the broadband noise data bank, and (4) a calculation procedure so that the program input deck can be modified to account for impulse signals of single rotor blade vortex interaction. The first three items are treated in this section, while the fourth item is treated in the Appendix.

ROTOR NOISE GROUND REFLECTION

The reflection of rotor noise from the ground surface is an important effect when evaluating helicopter acoustic emissions. Interaction of the reflected acoustic signal with the direct acoustic signal (the unreflected signal) can produce significant distortion of the emission, both in frequency and in magnitude. The reflected signal must travel a greater distance than the direct signal and therefore arrives at the microphone later than the direct signal. This time delay is an important parameter when evaluating the effects of ground reflection. To illustrate, Figure 1 shows an addition process for identical signals, the only difference being the ratio of the signal width to the time delay. When the signal width is 5 units and the time delay is 2 units, the addition process yields a slightly wider signal with increased magnitude. When the signal width is 2 units and the time delay is 5 units, the addition process yields two separate signals with the same magnitude. The end results of these two signal addition processes are obviously entirely different.

The ground reflection effect for helicopter rotor noise has been discussed extensively in References 3 and 4. Summarizing the results of the ground reflection calculation presented in Reference 3, the reflected and direct wave are in phase and add for the frequencies

$$f_a = c \, \frac{\sqrt{h^2 + d^2}}{2 \ell h} \, n \tag{1}$$

where f_a = frequencies at which the reflected signal is in phase with the direct signal (Hz)

    c = speed of sound (ft/sec)

    h = altitude of noise source (ft)

3

$\underline{d}$ = distance of microphone from source along the ground

$\underline{\ell}$ = microphone height (ft)

n = non-negative integer

The reflected and direct signals are 180° out of phase and cancel for the frequencies

$$f_c = c \frac{\sqrt{h^2 + d^2}}{2\ell h}(n + 1/2) \qquad (2)$$

where f_c = frequencies at which the reflected signal is 180° out of phase with the direct signal (Hz).

As mentioned previously, ground reflection is an important effect when evaluating the acoustic emissions of helicopter rotors. Figures 2 and 3 represent noise spectra of the UH-1B in a 100-ft hover created from data recorded at microphone positions 4 and 6 (see Figure 4). The spectra were generated by RASA's analysis system. The bandwidth is 0.7 Hz over the frequency range of 0 to 5600 Hz. Comparison of these two figures reveals that ground reflection is effective over different frequency ranges. Microphone 4 was located on concrete while microphone 6 was located on grass; yet microphone 6 exhibits the ground reflection phenomenon at higher frequencies, which is not as expected. Each spectrum shows approximately eight destructive interference regions (see Equation 2). The noise level drop from peak to valley is a measure of the effectiveness of the ground reflection phenomenon, but not necessarily a good measure because of differences in the background noise level and the magnitude of helicopter noise present at a particular frequency.

The noise level drop at position 4 for the first minimum (100 Hz) and at position 6 for the first minimum (350 Hz) is approximately 20dB. Assuming that the background noise level at these two minima is less than 40 dB (see Figures 2 and 3), the effectiveness of the reflection process may be calculated. The effectiveness of the reflection process may be expressed in terms of a ground reflection coefficient which modifies the magnitude of the reflected signal (1.0 is the maximum value of the ground reflection coefficient corresponding to perfect reflection). Since the noise level drop at the first frequency minima for the signals of Figures 2 and 3 is 20 dB each, the ground reflection coefficient for these two minima is 0.9.

4

The calculated value of the ground reflection coefficient is affected by the background noise level as well as the intensity of the source noise, and therefore, the noise level drop method described above establishes only the lower limit for the ground reflection coefficient. Hence at position 4 the ground reflection coefficient is at least 0.9 at 100 Hz; while at position 6, the ground reflection coefficient is at 0.9 at 350 Hz. Similar calculations may be undertaken at each of the ground reflection minima to establish the lower limit values of the ground reflection coefficient with frequency, but this process does not establish the true value of the ground reflection coefficient. To illustrate this discrepancy, Figures 2 and 3 indicate a smaller ground reflection coefficient with increasing frequency since the noise level drop decreases with increasing frequency, but the noise emitted from the source also decreases with increasing frequency and cancellation can occur only to the level of the background noise.

Detailed study of available spectra of helicopter rotor noise indicates that ground reflection coefficients are primarily affected by microphone height. Spectra with a microphone height exceeding 20 ft failed to show the ground reflection effect. The effect becomes more important with decreasing microphone height. The data available has not been sufficient to define precisely the values of the ground reflection coefficients as functions of surface conditions, source frequency, directivity, and source height. The data has indicated only a strong dependence on microphone height.

Using the available spectra, noise level drops have been measured for data recorded at various microphone heights to establish a formulation for the ground reflection coefficients as a function only of microphone height. The data indicates that

$$GRC = 1.0 \text{ for } \ell < 6 \text{ ft}$$

$$GRC = \exp\left[2.0\left(\frac{\ell}{\ell_{max}}\right) - 6.8\left(\frac{\ell}{\ell_{max}}\right)^2\right] \tag{3}$$

$$\text{for } 6 < \ell < 20 \text{ ft}$$
$$GRC = 0.0 \text{ for } \ell > 20 \text{ ft}$$

where

$$GRC = \text{ground reflection coefficient}$$

$$\ell = \text{microphone height}$$

$$\ell_{max} = 20 \text{ ft}$$

5

These calculations were made from data in which rotor-microphone orientation was such that small angles existed between the direct and reflected wave (for small angles the direct and reflected wave are identical) and minimal increases in travel distance of the reflected wave. Since rotor noise is highly directional, a large angle between the direct and reflected ray would indicate that the reflected ray is entirely different from the direct ray. Large increases in travel distance of the reflected ray when compared to the direct ray distance would cause the reflected ray to diminish in magnitude (spherical spreading), thereby reducing the overall effect of ground reflection. Significantly increasing the travel distance of the reflected ray relative to the direct ray is partly the explanation for the higher microphones not showing the ground reflection effect.

The noise prediction program developed under Contract DAAJ02-71-C-0064 calculates emitted acoustic pressures in a time frame, keeping proper account of rotor blade positions and velocities. The ground reflection phenomenon can therefore be represented by a time delay calculation which determines the time of arrival at the observer's location of not only the direct ray but also the reflected ray, with the magnitude of the reflected ray being modified by the ground reflection coefficient. The time delay is the increase in travel distance of the reflected ray divided by the speed of sound.

In the program, the rotor blades are divided into stations, each station having an aerodynamic force associated with it. The aerodynamic force is transformed into an acoustic signal received at an observer's location. Since each station has its own geometry relative to the observer's location, it also has an individual delay time for the reflected ray relative to the direct ray. The emitted pressures are summed at the observer's location with proper consideration for the delay time associated with each blade station. The ground reflection effect will therefore be included in the pressure time history, and any spectrum generated from the pressure time history will also have the ground reflection effect included.

VARIABILITY OF OSCILLATORY FORCES AS RELATED TO THE VORTEX SHEDDING PHENOMENON

Analysis of tapes generated in the previous programs (References 3 and 4) has indicated that variability in noise from blade passage to blade passage is an important effect when subjective evaluations are being conducted. The analysis done to date has assumed that the rotor aerodynamics (which govern the rotor noise output) do not change from blade passage to blade passage, so the problem could be made tractable. That is to say, the azimuthal distribution of blade loading can be specified by the user, but once defined, the aerodynamics are invariant with time. This assumption has not significantly limited the scientific content of the prediction program results, but it has reduced the "realism" of the acoustic tapes generated. This variability is most apparent in the broadband noise associated with discrete vortex shedding from the airfoil when the helicopter is in hover. Noise variability is best described by referring to Figure 5, taken from Reference 3. As the title indicates, the figure shows histograms of the magnitudes of the oscillatory lift forces calculated over the rotor blade from experimental data for a UH-1R in hover. These oscillatory lift forces are those assumed to be induced by vortex shedding. The variation in the oscillatory pressures reflects the signal variation from blade passage to blade passage. The first station is at a radius of 7 ft, while the tenth station is at the blade tip. Observe that the variability is significant. It has been demonstrated that this variability is very important in subjective evaluations and must be included if any degree of realism is to be achieved.

The mean values of the oscillatory lift forces can be determined from blade section values as a result of the work reported in Reference 4. This effort allowed the parameterization of the oscillatory lift forces determined from experimental data. Based on available data, the magnitude of oscillatory forces increases with angle of attack and decreases with section velocity. The parameterization that was developed is given by

$$P_{osc} = 2 \ (1-M) \ [1 + (\tfrac{\alpha}{4})^2]$$

where P_{osc} is the oscillatory section pressure (lb/ft^2)

      M is the section Mach number >0

      α is the section angle of attack (deg)

7

The parametric fit for the oscillatory force constants was undertaken for a Strouhal number, independent of section variables, equal to 0.235, which was determined as the best fit for vortex shedding induced noise (Reference 3). The above formulation was used in the predictive program presented in Reference 4, whose results correlated well with experimental results.

The present predictive program (Reference 4) assumes that the rotor is operating such that the angle of attach and Mach number at a given blade radial and azimuthal station are invariant from blade passage to blade passage. This assumption is consistent with current rotor aerodynamic theory for a rotor operating in either hover or steady-state forward flight. It is recognized, however, in actuality that these parameters do vary. It is believed that this variation is attributable to a number of causes, such as perturbations in wind velocity or local turbulence and deviations from true idealized steady-state conditions associated with changes in trim and attitude.

Equation 4 relates the strength of oscillatory pressure at a blade element to local blade element angle of attack and Mach number, and assumes that for a given blade position these values do not change with time. However, as has been discussed, it is recognized that even in the hover condition, both blade element angle of attack and Mach number do vary at a given point on the rotor disk. It is believed that this variation gives rise to the changes noted in the calculated oscillatory pressures where test data served as the base (References 3 and 4). The variability from blade passage to blade passage of the blade section parameters is not known, since as has been discussed it depends upon the random occurrences of a number of variables. Since measured data indicates that oscillatory forces do vary from blade passage to blade passage in both frequency and magnitude, the variation in noise signature was introduced in the analysis by allowing each oscillatory force of frequency ω to vary about its mean values in a random fashion within bounds consistent with results shown in Figure 5. The time scale for the variation is in the range of periods expected for main rotor blade passages.

EXPANSION OF THE DATA BASE FOR THE BROADBAND NOISE DATA BANK

The work discussed in this section is an extension of the fundamental work conducted previously and reported in Reference 4. In that effort, an expression was developed for the aerodynamic forces on the rotor blades that produce broadband or vortex noise (see Equation 4). The noise data that was used

to generate that equation was recorded from a CH-47B rotor
and a modified H-19 rotor, both of which were mounted on
whirl towers. The objective of the present effort was to ex-
pand the data base for the previously derived equation. The
forces on the rotor blade that generate broadband noise have
been assumed to be those induced by discrete vortex shedding
at frequencies determined by a Strouhal calculation
(Reference 3). The vortex shedding frequencies of the rotor
blade sections are not related to the blade passage fre-
quency of the rotor. An array of forces at the rotor blade
sections oscillating at individual frequencies moving with
the rotor blade produces a broadband signature at the ob-
server location, but this random signature is modulated by
the rotor passage frequency. With the frequency of the os-
cillatory forces known from the Strouhal calculation, the
magnitude of the oscillatory forces can be determined as
functions of the section Mach number and angle of attack from
controlled rotor acoustic tests conducted on a whirl tower.
The magnitudes can then be parameterized as functions of the
section variables such as Mach number and angle of attack.
This procedure defines a "data bank": a relation containing
information concerning vortex noise that was reduced from
experimentally recorded acoustic records. The basic proce-
dure used to determine the magnitudes of the oscillatory
force constants is as follows:

1. Blade-element momentum theory is used to determine
   the distribution of angles of attack and flow
   velocity across the whirl tower rotor blade for a
   thrust value equal to that attained for the re-
   corded acoustic data.

2. These angles of attack and flow velocities are
   then used to determine the vortex shedding fre-
   quency by

$$\omega = \frac{S_t u}{th} \tag{5}$$

where ω = vortex shedding frequency

   th = blade section thickness as seen by the
        flow (for most helicopter blades, th
        equals blade thickness since the aero-
        dynamic angle of attack rarely exceeds
        7 degrees)

   u = flow velocity

   S_t = Strouhal number

9

The Strouhal number is set equal to 0.235 and is held independent of section variables. This Strouhal number was determined as the "best fi⌐" during the research investigation reported in Reference 3.

3. A 1-ft spanwise station at mid-span and one at the blade tip are given an oscillatory pressure of 1 lb/ft^2 in the lift direction. (The oscillatory drag is set equal to zero since acoustic data taken in the plane of the rotor indicated that very little noise is produced by vortex shedding in that direction.) For each of the 1-ft-wide stations, a pressure time history was predicted at an observer location appropriate to the recorded data.

4. The predicted pressure time histories are then Fourier analyzed and compared to the spectrum of the experimental data in the appropriate frequency range. The oscillatory force magnitude at each of the blade stations is adjusted so that the predicted spectrum and experimental spectrum have the same magnitude in the appropriate frequency range.

This process yields two oscillatory pressures in the lift direction for different angles of attack and Mach numbers. Repetition of this process for different rotor configurations and other blade stations yields an array of oscillatory pressures which are then parameterized as functions of angle of attack and Mach number.

The acoustic signatures used to expand the data base for the broadband noise data bank were recorded by NASA-Langley during their recent whirl tower tests. The whirl tower acoustic recordings were made using an XH-51 rotor. The rotor has four blades, a radius of 17.5 feet, a chord of 13 inches and a twist of -5°. The tip speeds recorded were 277, 412, 478, and 649 ft/sec. The thrust ranged from 1548 lb to 10,100 lb.

Certain records from the XH-51 data were analyzed for use in expanding the data banks (see Table I). Table I lists the rotor microphone locations, the rotor operating conditions, and the rotor geometric parameters. The analysis of this data failed to show any changes in the parametric formula (Equation 4) representing rotor broadband noise developed previously in Reference 4. Since the present relationship satisfactorily represents the broadband noise produced by the XH-51 rotor, no changes were made in Equation 4. In summary, the parametric formula that has been developed satisfactorily represents the broadband noise produced by the following rotors: CH-47B, UH-1B, H-19, and XH-51.

10

TABLE I. XH-51 WHIRL TOWER TEST CONDITIONS USED IN THE DATA BANK

Record Source	Rotor Height (ft)	Microphone From Rotor Axis (ft)	Microphone Height (ft)	Thrust (lb)	Tip Speed (ft/sec)	Number of Blades	Blade Radius/Chord (ft)/(in.)
NASA (XH-51)	45	150	4.25	1550	277	4	17.5/13.
	45	150	4.25	3400	412	4	17.5/13.
	45	150	4.25	1548	478	4	17.5/13.
	45	150	4.25	4750	649	4	17.5/13.
	45	150	4.25	10100	649	4	17.5/13.

RESULTS - TEST CASES

In order to evaluate the accuracy of the additional features
of the rotor acoustic prediction program, several test cases
were devised. The first test of the extended prediction tech-
nique was to determine its capability of predicting rotor
noise with proper consideration for the ground reflection
phenomenon. This test was carried out for the UH-1B helicopter
in level flight. The next test of the program was to determine
its ability to introduce variation in the acoustic signature
from blade passage to blade passage. This test was conducted
for a UH-1D main rotor in hover. The final test of the pro-
gram was to demonstrate that the acoustic effects of blade
vortex interaction can be predicted with proper aerodynamic
input to the program. This test was conducted for a UH-1D
main rotor in level flight.

GROUND REFLECTION - UH-1B IN LEVEL FLIGHT

To demonstrate that the acoustic program can accurately pre-
dict the effects of ground reflection, a prediction of the
noise output of the UH-1B in forward flight was conducted. The
UH-1B helicopter was chosen for these predictions, as exten-
sive, well documented noise data exist for this helicopter (see
Reference 3). The acoustic prediction conducted herein can be
compared to the data recorded at microphone position 4 for the
122-knot flyby at 100 ft (see Figure 4).

Additional specifications supplied by the Army for the UH-1B
are: the main rotor has two blades (NACA 0012) with a radius
of 22 ft and a chord of 21 in.; the rotational speed is 324
rpm. The tail rotor also has two blades (NACA 0015), but with
a radius of 4.25 ft and a chord of 8.4 in.; the rotational
speed is 5.108 times that of the main rotor, or 1655 rpm.

The spectrum of the experimental noise was generated when the
helicopter was 1160 ft uprange and is shown in Figure 6. It
has been shown that a noise spectrum of a moving helicopter
is meaningful if the helicopter-observer orientation does not
change significantly (see Reference 3) for the time period
required to generate the spectrum. Since the length of the
data record used to generate the spectrum was only 1 second
and the helicopter position was far uprange, the helicopter-
observer orientation could not change significantly and the
spectrum presented in Figure 5 is meaningful. In Figure 6,
note that the first ground reflection minimum occurs at 560
Hz, which confirms the reported position of the helicopter
(see Equation (2)). The main rotor rotational noise is
significant to 300 Hz, and the tail rotor rotational noise
is significant to 1400 Hz.

12

The noise prediction was generated using the helicopter flight conditions and observer location as defined by the experiment (see Reference 3). The predicted spectrum is shown in Figure 7. Both the experimental and predicted spectrums have 1-Hz bandwidths. Note that the ground reflection minimum occurs at 560 Hz in the predicted spectrum as in the experimental spectrum. As the helicopter approaches the observer, the ground reflection minima will decrease in frequency, thereby creating important subjective effects. The predicted main rotor noise levels compare quite well with the experimental main rotor noise levels. The predicted tail rotor noise is 4 db too low around 300 Hz and about 6 db too high around 800 Hz. It is believed that this discrepancy is caused by insufficient information concerning the coefficient of drag for the NACA 0015 airfoil at high Mach numbers. The airfoil tables used were derived from NACA Report No. 832 (Reference 5). These tables contain information up to $M = 0.825$. The tail rotor tip speed, however, reaches $M = 0.86$. The prediction program extrapolates beyond the highest table value, but this procedure may not reflect the true physical dependence of the NACA 0015 coefficient of drag with Mach number since the drag curve slope is very steep around $M = 0.85$. This situation does not arise for the main rotor since the main rotor is an NACA 0012 and these airfoil tables cover Mach numbers up to $M = 1.0$.

In order to demonstrate the changes in the noise pressure time history during the flyby, comparisons will be made of the predicted and experimental pressure time histories at different helicopter locations during the flyby. Figure 8 shows the predicted and experimental pressure time histories when the helicopter is at $X = -900$ ft (see Figure 4). The main rotor rotational noise pulses are larger than the tail rotor rotational noise pulses. The tail rotor pulses occur approximately 5 times the main rotor pulses (the tail rotor rotational speed is 5.108 times that of the main rotor). Note the double peaks of the tail rotor rotational noise pressure pulses. These double peaks are caused by ground reflection; the separation distance between the double peaks increases as the helicopter approaches. Figure 9 shows the comparable noise prediction without ground reflection. Note that there are no double peaks in the tail rotor signature. Note also in Figure 9 that the main rotor signature appears equal in magnitude to the tail rotor signature, while in Figure 8 the main rotor signature is larger than the tail rotor signature. This difference is also caused by ground reflection. The main rotor signal is amplified by ground reflection because it is wider than the tail rotor signal (see Figure 1). The next three plots (Figures 10, 11, 12) repeat the format of Figure 8, but for the helicopter at -700, -500, and -350 ft respectively.

13

It can be seen that the separation in the double tail rotor pulses increases as the helicopter approaches the observer in both the predicted and experimental traces.

The predicted noise tapes for the UH-1B flyby are realistic when compared to the experimental tapes. The main rotor and tail rotor rotational noise levels and frequencies are accurately predicted (the predicted tail rotor noise is slightly louder than the experimental tail rotor noise). The main rotor/tail rotor beating phenomenon is also evident (tail rotor rotational speed is 5.108 times the main rotor rotational speed). The Doppler shift as the helicopter flies past the observer is present in the predicted tapes, and the vortex noise sounds like the broadband noise heard in the experimental tapes.

VARIABILITY OF ROTOR NOISE - UH-1D IN HOVER

The test for variability of rotor noise was conducted for a UH-1D main rotor in hover. This test was completely subjective. The addition of the random process which varies the broadband noise parameters about their calculated mean values has not disturbed the noise prediction accuracy but has made the tapes sound "much more like a helicopter" when the flight mode is in hover. This process is not needed in rectilinear flight, as the variability in noise from blade passage is much less important subjectively.

Figure 13 shows two blade passages of UH-1D main rotor predicted pressure time history with and without the noise variability option. Without the variability option, the noise signature from blade passage to blade passage does not change significantly. With the variability option, the noise does change from blade passage to blade passage, which is typical of experimental noise records.

BLADE SLAP - UH-1D IN LEVEL FLIGHT

The test for blade slap was conducted for a UH-1D main rotor in level flight. Since blade slap is a form of rotational noise, it is not necessary to include broadband noise in the prediction. Two predictions were carried out: one with the effects of a concentrated tip vortex interacting with the blades as represented by the aerodynamic input to the noise prediction program, and one without the effects of a concentrated tip vortex. The helicopter position is 1600 ft uprange and 1000 ft high. The microphone is 450 ft to the right of the flight path. The forward velocity is 25 kt, which corresponds to the flight conditions associated with the lobe for blade slap seen in Figure 14, taken from Reference 6. Note that this particular flight condition is not a dominant blade slap

14

case. Hawles (Reference 6) calls this particular form of
blade slap "continuous slap" (see Figure 14). The aerody-
namic input for the blade vortex interaction case was
calculated using the principles established in the Appendix.
The predicted pressure time histories are shown in Figure 15.
Note the double spike for the blade slap case which is typical
of a blade vortex interaction. The case without the tip vor-
tex shows just the standard rotational noise. These
predictions clearly demonstrate that the acoustic effects of
a blade vortex interaction can be predicted provided the pro-
per aerodynamic input is supplied to the prediction program.

CONCLUSIONS AND RECOMMENDATIONS

This program has resulted in the successful development of a design tool that realistically predicts helicopter rotor noise. The design tool has the capability of evaluating the acoustic characteristics of new, untested rotor designs as well as the effects of basic rotor design changes on the acoustic signature of existing rotors. The computer design tool should find popular use in the Government as well as the helicopter industry because the predictions are accurate and the program inputs are just the geometric and aerodynamic parameters of the helicopter rotor system. One of the most important features of this tool is that only a digital-to-analog conversion is required in order to evaluate the helicopter noise prediction subjectively.

The following specific conclusions are drawn:

1. Rotational noise is predicted accurately.

2. The parameterization of the oscillatory forces accurately represents the broadband noise over the range of parameters normally encountered in specifying helicopter rotor systems.

3. The program can predict the noise resulting from blade vortex interactions provided the proper aerodynamic information is supplied as input to the program.

4. Ground reflection effects distort the radiated acoustic pressure-time history, and this distortion is particularly important subjectively. Ground reflection effects are properly considered in the prediction program.

5. The variability of broadband noise from blade passage to blade passage in a hover configuration is also important in subjective analysis. This effect is also included in the prediction program.

6. Near-field noise is predicted as well as far-field noise.

7. The predicted noise may be evaluated in any one of three ways:
   1) pressure time history,
   2) spectra,
   3) audio tapes.

8. The program is applicable to propellers as well as rotors.

9. The broadband and rotational noise can be investigated independently.

10. A combination of rotors can be investigated simultaneously.

11. The program can predict the noise from an aircraft in hover or in rectilinear flight.

It is recommended that an effective demonstration of the rotor noise prediction program's capabilities be conducted so that the program will be used in industry and Government. The ideal approach for this demonstration is to conduct a prediction with each of the helicopter manufacturers for a helicopter of interest, so that the manufacturers may evaluate the program's capability with a familiar aircraft. This process would also serve to familiarize the manufacturer with the prediction program. The ultimate goal is to find a universal approach to helicopter rotor acoustics in Government and industry.

17

REFERENCES

1. Lowson, M.V., THE SOUND FIELD FOR SINGULARITIES IN MOTION, Proceedings of the Royal Society, A. Vol. 286, pp. 559-572,1965.

2. Lowson, M.V., Ollerhead, J.B., STUDIES OF HELICOPTER ROTOR NOISE, USAAVLABS Technical Report 68-60, U.S. Army Aviation Materiel Laboratories, Fort Eustis, Virginia, January 1969, AD 684394.

3. Johnson, H. Kevin, Katz, Walter M., INVESTIGATION OF THE VORTEX NOISE PRODUCED BY A HELICOPTER ROTOR, USAAMRDL Technical Report 72-2, Eustis Directorate, U.S. Army Air Mobility Research and Development Laboratory, Fort Eustis, Virginia, February 1972, AD 741778.

4. Johnson, H. Kevin, DEVELOPMENT OF A TECHNIQUE FOR REALISTIC PREDICTION AND ELECTRONIC SYNTHESIS OF HELICOPTER ROTOR NOISE, USAAMRDL Technical Report 73-8, Eustis Directorate, U.S. Army Air Mobility Research and Development Laboratory, Fort Eustis, Virginia, March 1973.

5. Graham, Donald J., Nitzberg, Gerald E., Olson, Robert N., A SYSTEMATIC INVESTIGATION OF PRESSURE DISTRIBUTIONS AT HIGH SPEEDS OVER FIVE REPRESENTATIVE NACA LOW-DRAG AND CONVENTIONAL AIRFOIL SECTIONS, Report No. 832, Ames Aeronautical Laboratory, National Advisory Committee For Aeronautics, Moffett Field, Calif.

6. Hawles, D., FLIGHT OPERATIONS TO MINIMIZE NOISE, Vertiflite, Vol. 17, No. 2, February 71, pp. 4-9.

7. Evans, T.D., FINDING THE IN-PLANE POINT OF BLADE/VORTEX INTERSECTION, RASA Inhouse Memo, 12 August 1973.

8. Evans, T.D., SOLUTION OF THE EXACT EQUATIONS BY NEWTON'S METHOD, RASA Inhouse Memo, 12 August 1973.

9. Zalay, A., VORTEX INDUCED VELOCITY FIELD FOR A UH-1B ROTOR IN HOVER, RASA Inhouse Memo, 10 October 1972.

10. Evans, T.D., COMPUTATION OF THE INFLOW VELOCITY INDUCED BY A BLADE/VORTEX INTERACTION, RASA Inhouse Memo, 13 August 1973.

11. Evans, T.D., INTERSECTION OF A SHED VORTEX BY A HELICOPTER BLADE, RASA Inhouse Memo, 10 August 1973.

APPENDIX
HAND CALCULATION FOR INCLUDING SINGLE ROTOR BLADE VORTEX
INTERACTION IN THE AERODYNAMIC INPUT TO THE NOISE PROGRAM

The following procedure outlines a hand calculation which will
allow a previously generated aerodynamic input deck (to the
noise program) to be modified to include the effects of blade
vortex interactions. If the previously generated aerodynamic
input deck is the result of a detailed wake program that con-
siders the tip vortex, the hand calculation would obviously
not be required. The steps in the hand calculation are as
follows:

1. Determine whether or not the blade/vortex inter-
   action can be expected to produce significant noise.
   One method of doing this is to use Figure 14, taken
   from Reference 6. This figure gives the regions of
   blade slap. However, this figure can only be ap-
   plied to two-bladed, 10,000-lb class helicopters
   such as the UH-1. Similar information does not
   exist for different classes of helicopters. In any
   case, whether or not the phenomenon known as blade
   slap occurs, there will always be blade/vortex in-
   teractions, and these interactions can be expected
   to affect the blade loading and thus the noise
   signature in some way. Therefore, the following
   procedure can be used even when there is some doubt
   as to the significance of the effect on the noise
   signature.

2. Determine the inplane intersection points of the
   shed vortex with the blade. There are three ways
   of doing this. The easiest is to use the charts in
   Figure 16, taken from Reference 2. A second way is
   to use the following equation from Reference 7 (see
   Figure 17) for each azimuthal blade position ψ:

$$s = \cos T - \mu T \cos \psi + \mu \Phi \cos \psi \qquad (6)$$

where

$\quad$ s = radial station of intersection
$\quad$ ψ = azimuthal angle of intersecting blade
$\quad$ $T = \psi_1 - \psi \doteq \mu \Phi \sin \psi / (\mu \sin \psi + 1)$
$\quad$ ψ_1 = azimuthal angle of shedding blade
$\quad$ μ = advance ratio
$\quad$ Φ = azimuthal angle between shedding blade
$\qquad$ and intersecting blade

19

However, the second approach is accurate only for azimuthal spacings, ϕ, between the shedding blade and the intersecting blade $\leq 180^\circ$. For larger azimuthal separations, a third procedure may be used to locate the intersection points. This third procedure requires the solution of the equations used to generate the chart referred to previously (Figure 16). The actual equations given in Reference 2, however, are incorrect; the correct equations, from Reference 7, are:

$$T = \phi - \sin T/\mu \sin \psi \qquad \text{(a)}$$

$$s = \cos T - \mu T\cos \psi + \mu\phi\cos \psi \qquad \text{(b)}$$

(7)

Equations (7a) and (7b) are accurate for all ϕ. Equation (7a) may be solved for T by Newton's method as described in Reference 8. The other terms are defined under Equation (6).

3. Determine the vertical distance, h, of the vortex beneath the rotor. An estimate of this distance for level flight can be made by assuming that the vortex moves with the mean downwash velocity during the time it takes to move from the shedding blade to the intersecting blade. The angle T determined above is the difference between the azimuthal position of the shedding blade when it shed the vortex element being intersected, and the intersecting blade at the time of intersection. Physically, the intersecting blade follows the shedding blade at an angular distance ϕ (see Figure 17). Therefore, in the same time between shedding and intersection of the vortex element, the rotor has moved through an angle of $\phi + T$. If the angular velocity of the rotor is $2\pi\Omega/60$ rad/sec (Ω in rpm), then the time between shedding and intersection of the vortex element is

$$\Delta t = (\phi + T)/(2\pi\Omega/60)$$

If the vortex element moves downward with the mean downwash velocity $\overline{w}$ during this time, the vertical distance of the vortex beneath the blade at the point of inplane intersection is for level flight

$$h = \overline{w}(\phi + T)/(2\pi\Omega/60) \qquad (8)$$

For a descent flight condition, reduce $\overline{w}$ by the amount of the descent velocity.

20

4. Determine the strength of the tip vortex Γ. One way to estimate Γ is to assume a triangular loading on a blade such that the lift, $L = 0$ at $0.1R$, $L = L_{max}$ at $0.9R$. Then $\Gamma = \Gamma_{max}$ at $0.9R$, and applying the Kutta-Joukowsky law (see Reference 9),

$$\Gamma_{max} = L_{max}/\rho\Omega(0.9R)$$

$$L_{net} = 1/2(0.9R - 0.1R)L_{max}$$

$$= 0.4RL_{max}$$

$$\begin{cases} \Gamma_{max} = L_{net}/\rho\Omega(0.9R)(0.4R) \\[2mm] \Gamma_{max} = 2.78\ L_{net}/\rho\Omega R^2 \quad (\Omega \text{ in rad/sec}) \\[2mm] \Gamma_{max} = 26.547\ L_{net}/\rho\Omega R^2 \quad (\Omega \text{ in rpm}) \end{cases} \qquad (9)$$

5. Determine the downwash velocity induced on the blade by the tip vortex at each radial station x/R. From References 10 and 11,

$$u_z = \frac{\Gamma}{2\pi R}\ \frac{\left(\dfrac{x}{R} - s\right)\cos T}{\left(\dfrac{x}{R} - s\right)^2 \cos^2 T + (h/R)^2} \qquad (10)$$

where s = radial station of intersection (Equation (6)).

6. Determine the new downwash velocity by adding that determined from the preceding step to the downwash velocity determined from the user's aerodynamic programs at each radial station affected.

$$w_{new} = w_{old} + u_z \qquad (11)$$

7. Determine the new inflow angle at each radial station affected.

21

$$\phi = \tan^{-1}\left(w_{new}/v\right) \qquad (12)$$

where v is the total station velocity. The total station velocity must include the component of the helicopter forward velocity parallel to the blade motion due to rotation.

8. Determine the new effective angle of attack at each radial station affected.

$$\alpha_{eff} = \alpha_{geom} - \phi$$

9. The new lift and drag coefficients and, hence, the new blade loading can now be determined from airfoil section data.

This procedure must be repeated for every azimuthal position affected.

2/5

5/2
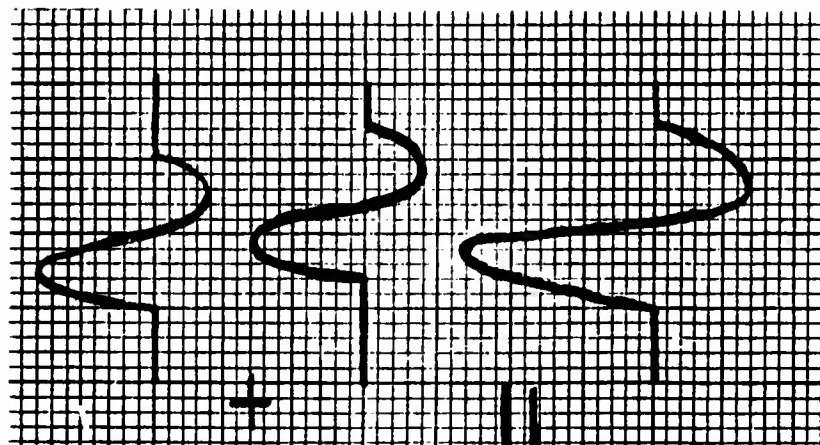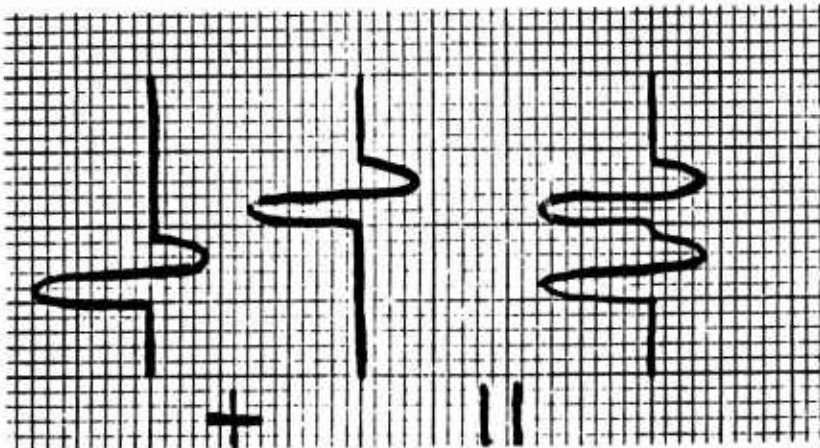
Figure 1. Acoustic Effects of Ratio of Pressure Pulse Width to Ground Reflection Time Delay.

23
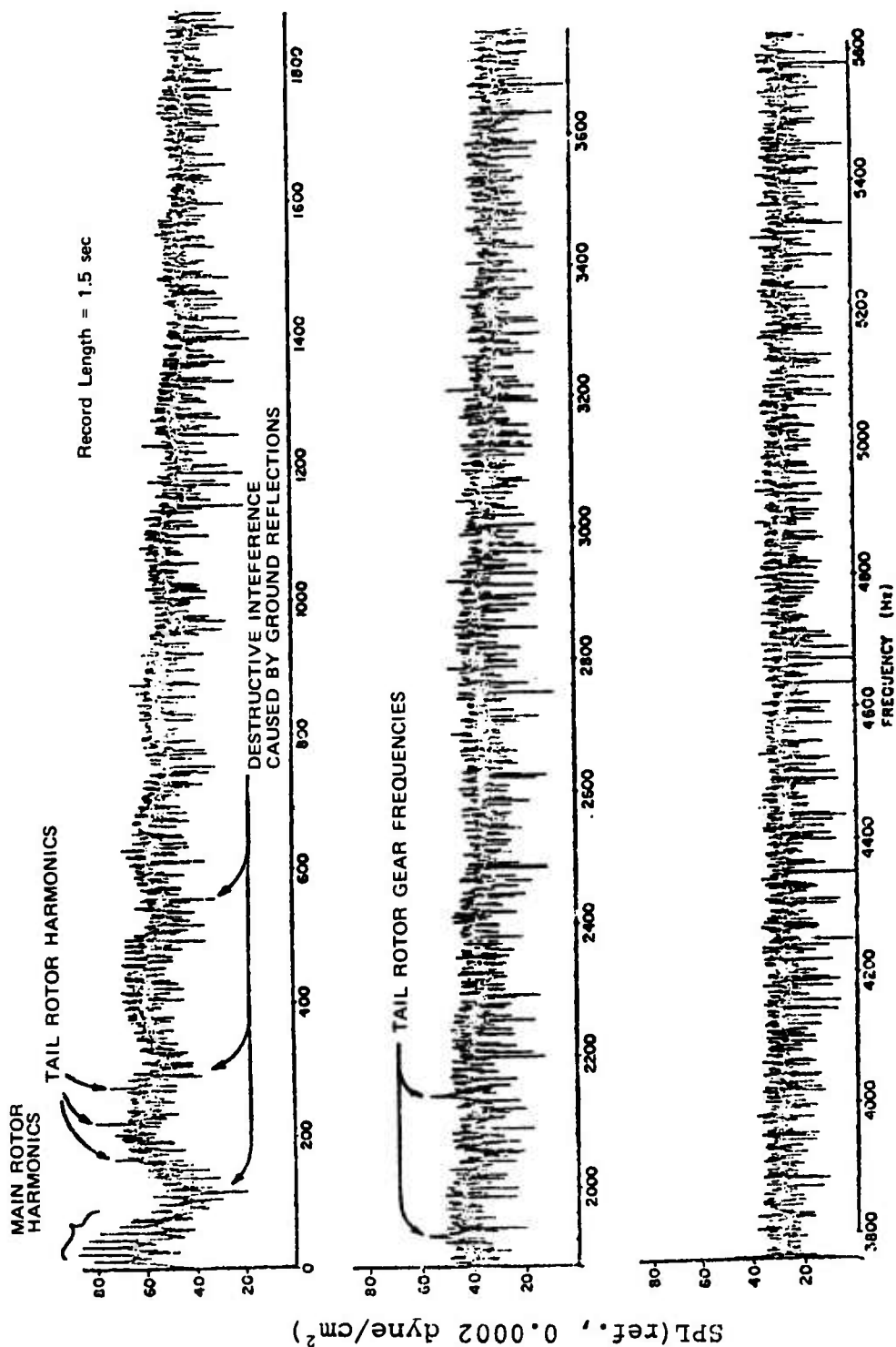
Figure 2. RASA Electronically Digitized Noise Spectrum for UH-1D in Hover; Recorded at 200 Ft to the Right; Data Taken 26 Seconds Into Record.

24
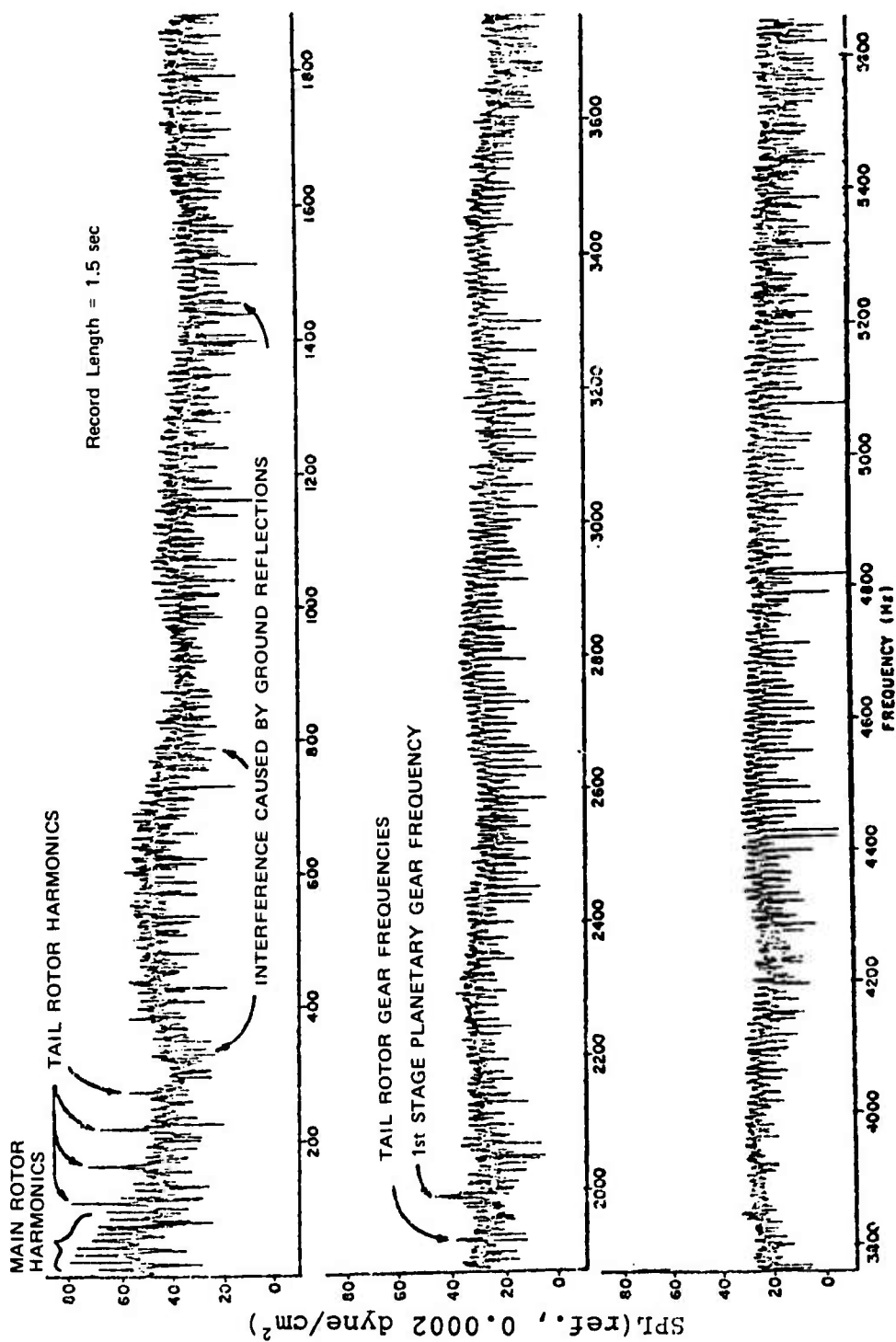
Figure 3. RASA Electronically Digitized Spectrum for UH-1B in 100-Ft Hover; Recorded at 700 Ft to the Right; Data Taken 26 Seconds Into Record.
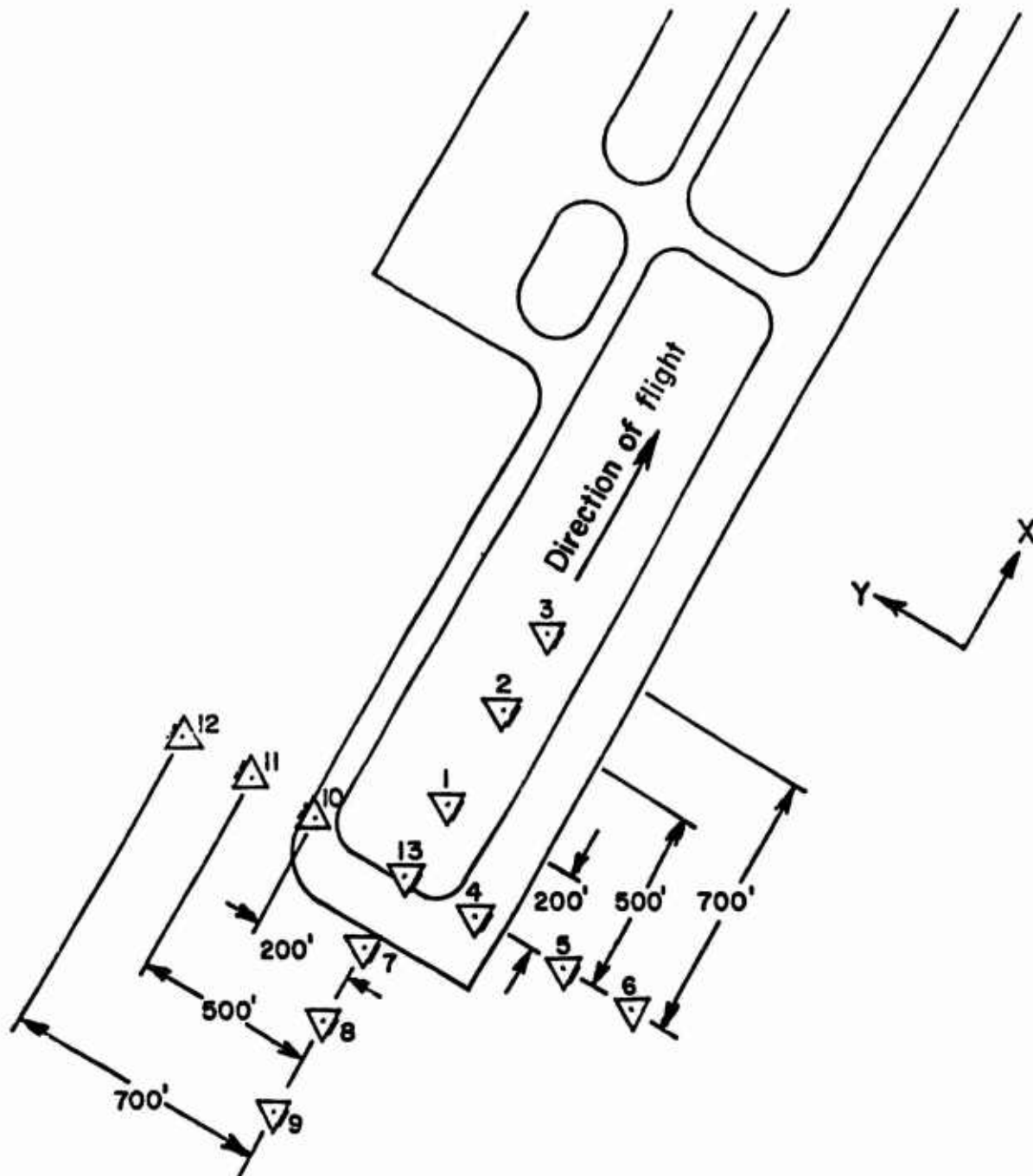
△ Microphone location and direction during flyby

Figure 4. Relative Positions of Microphones.
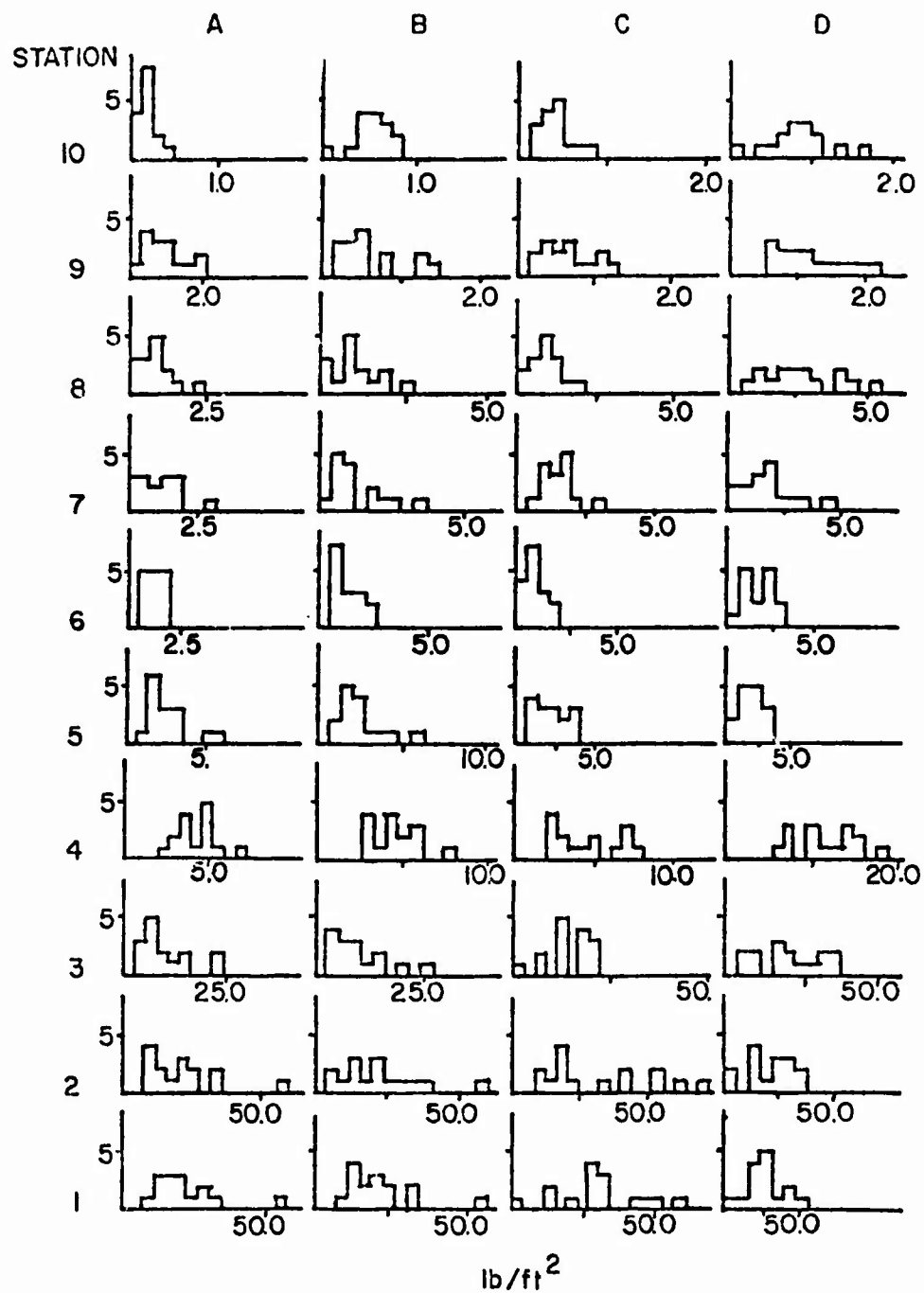
Figure 5. Distribution of the Magnitude of Oscillatory
Lift Over Ten Radial Stations for Four Cases.

27
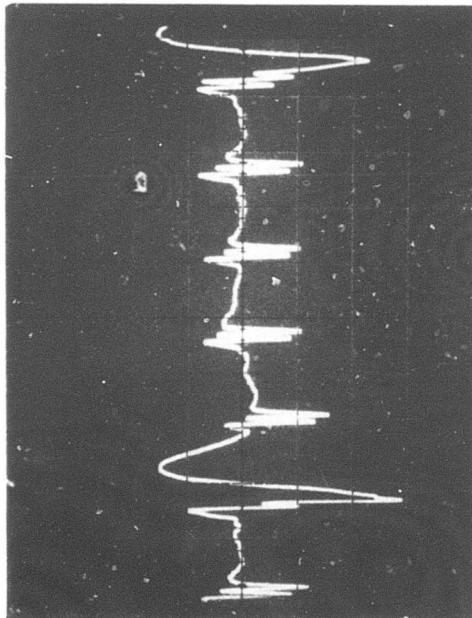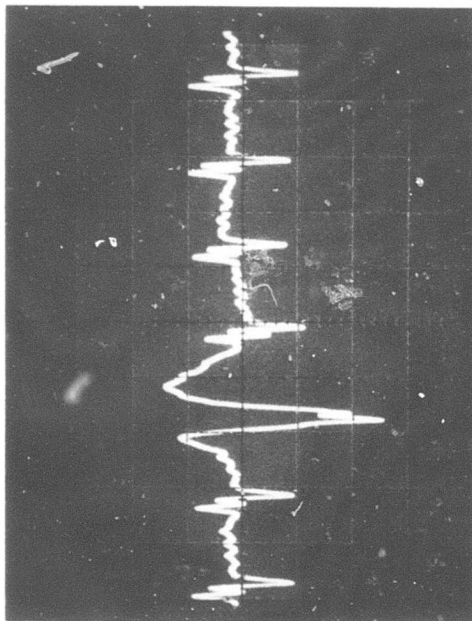
Figure 6. Spectrum of Recorded Noise Generated From a UH-1B in Level Flight.

28
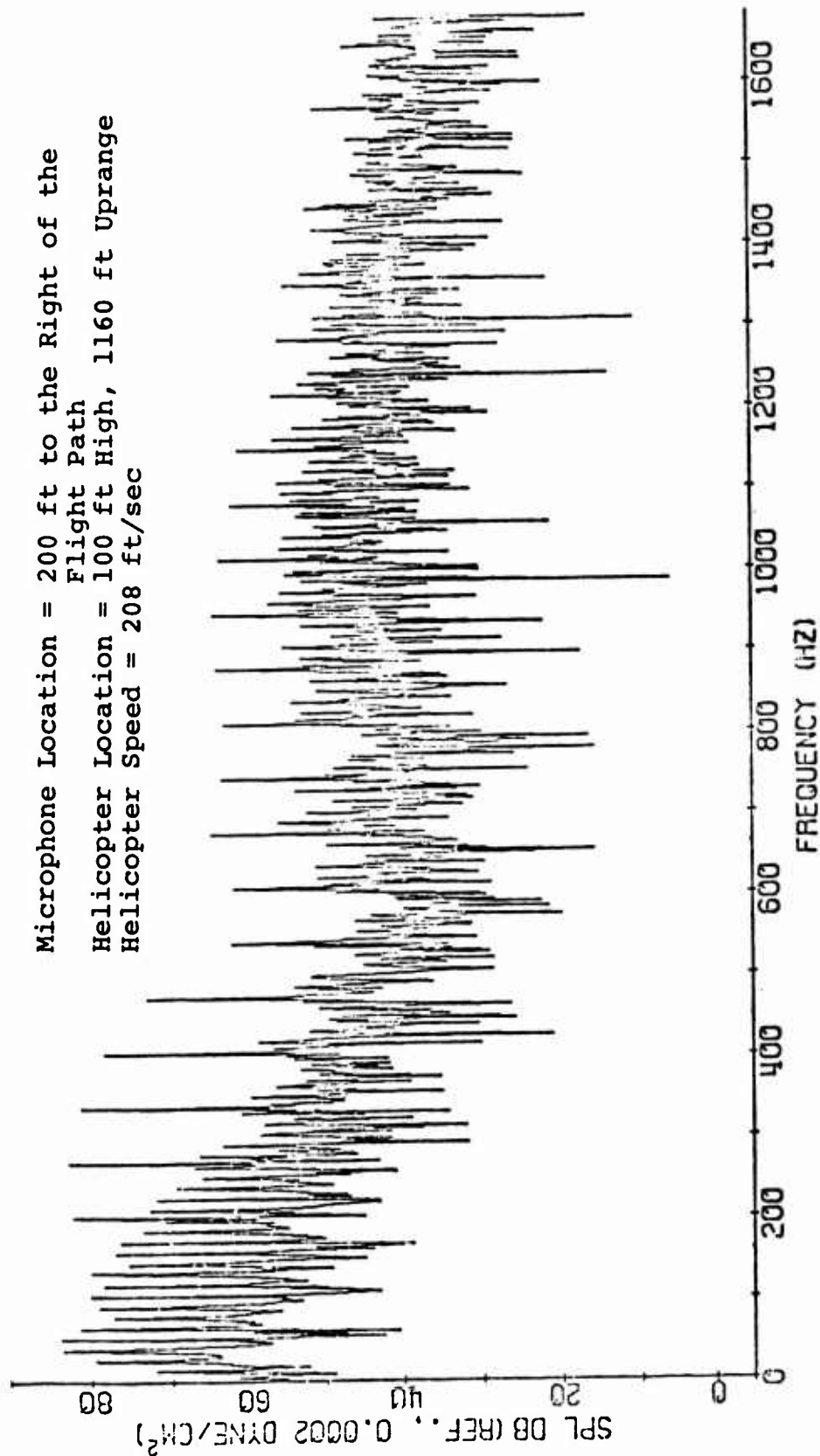
Microphone Location = 200 ft to the Right of the
Flight Path

Helicopter Location = 100 ft High, 1160 ft Uprange

Helicopter Speed = 208 ft/sec

SPL DB (REF.. 0.0002 DYNE/CM²)

FREQUENCY (HZ)
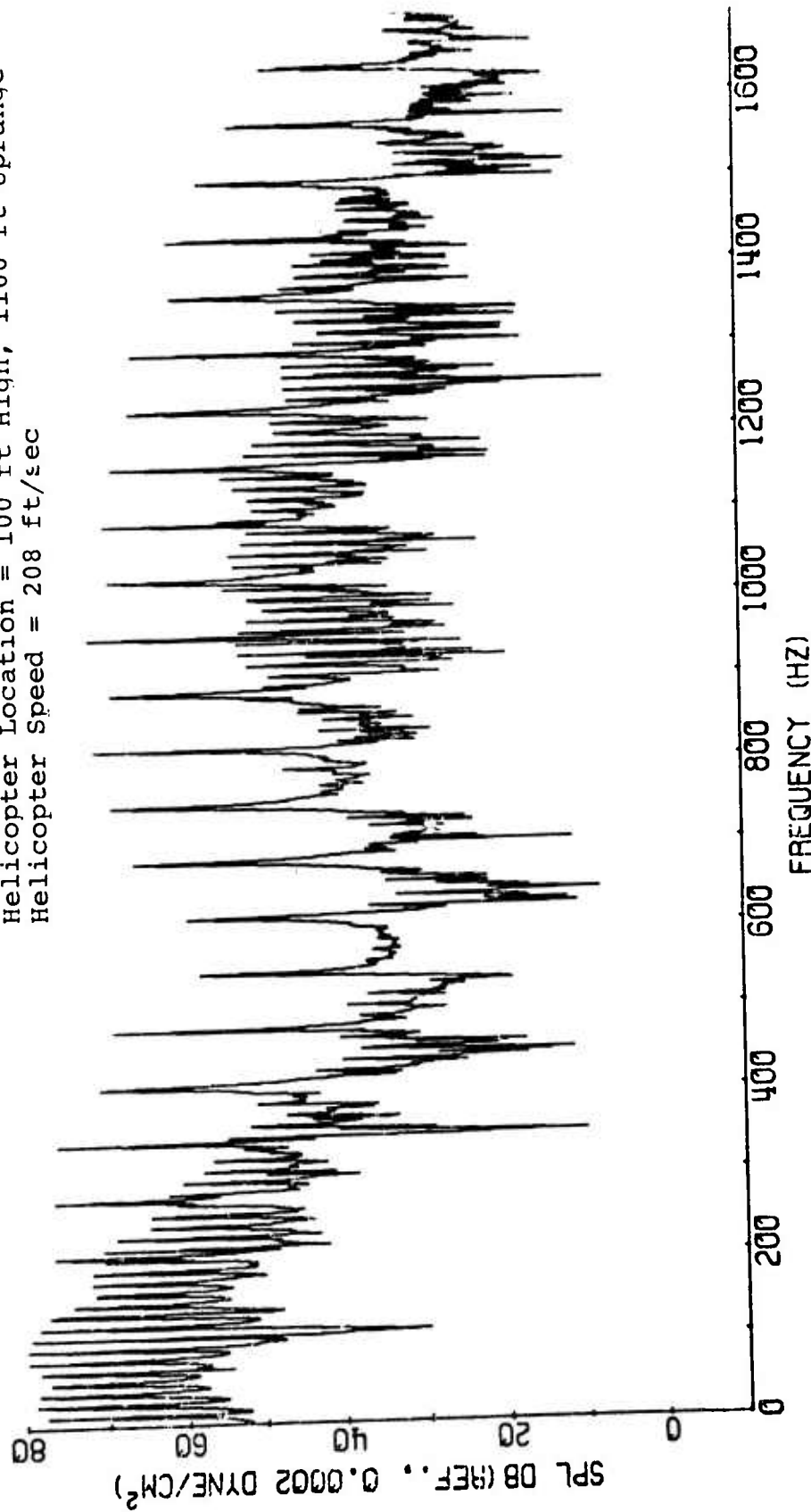
Figure 7. Spectrum of Predicted Noise Generated From a
UH-1B in Level Flight.

29

Microphone Location: 200 ft to the Right of the Flight Path
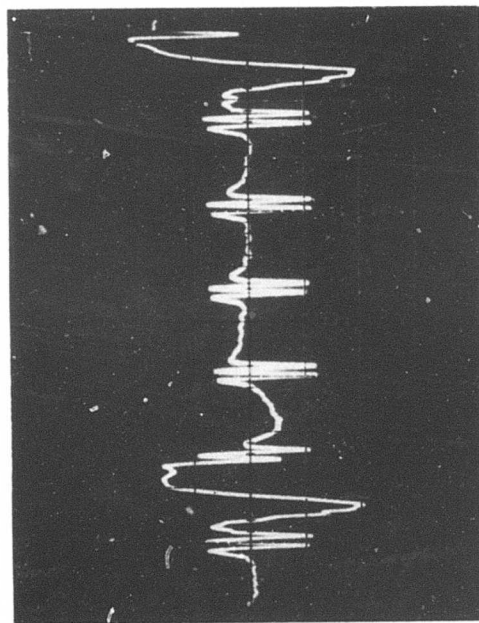Helicopter Location: 100 ft High, 900 ft Uprange
Helicopter Speed: 208 ft/sec
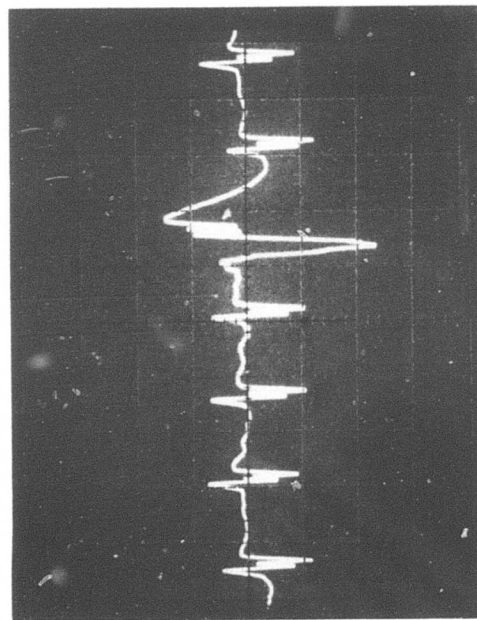
Experimental Pressure Time History
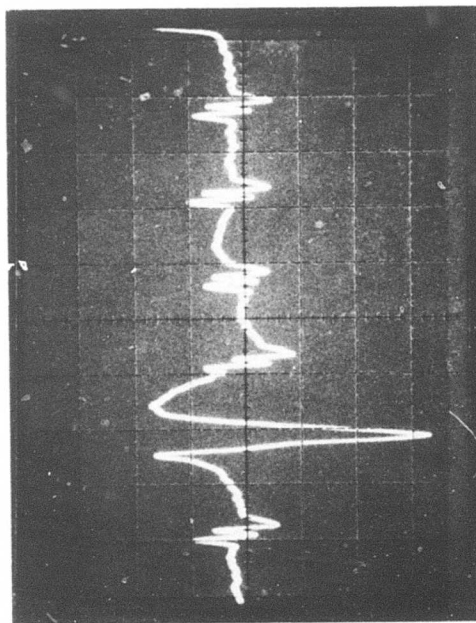Vertical Scale: 1 cm is 0.08 lb/ft^2
Horizontal Scale: 1 cm is 0.01 sec
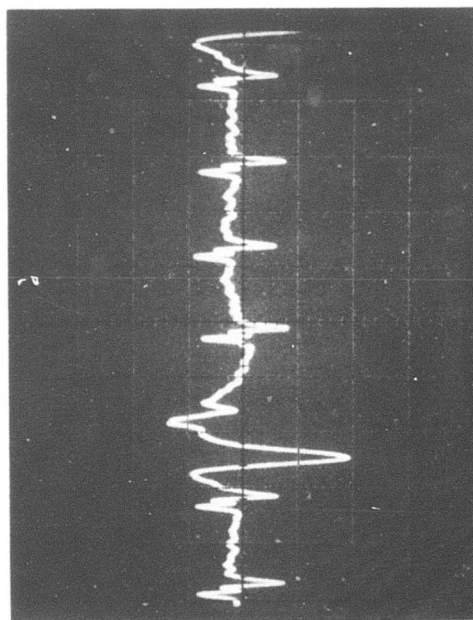
Predicted Pressure Time History
Vertical Scale: 1 cm is 0.06 lb/ft^2
Horizontal Scale: 1 cm is 0.01 sec

Figure 8. Pressure Time Histories of Noise From a UH-1B in Level Flight.
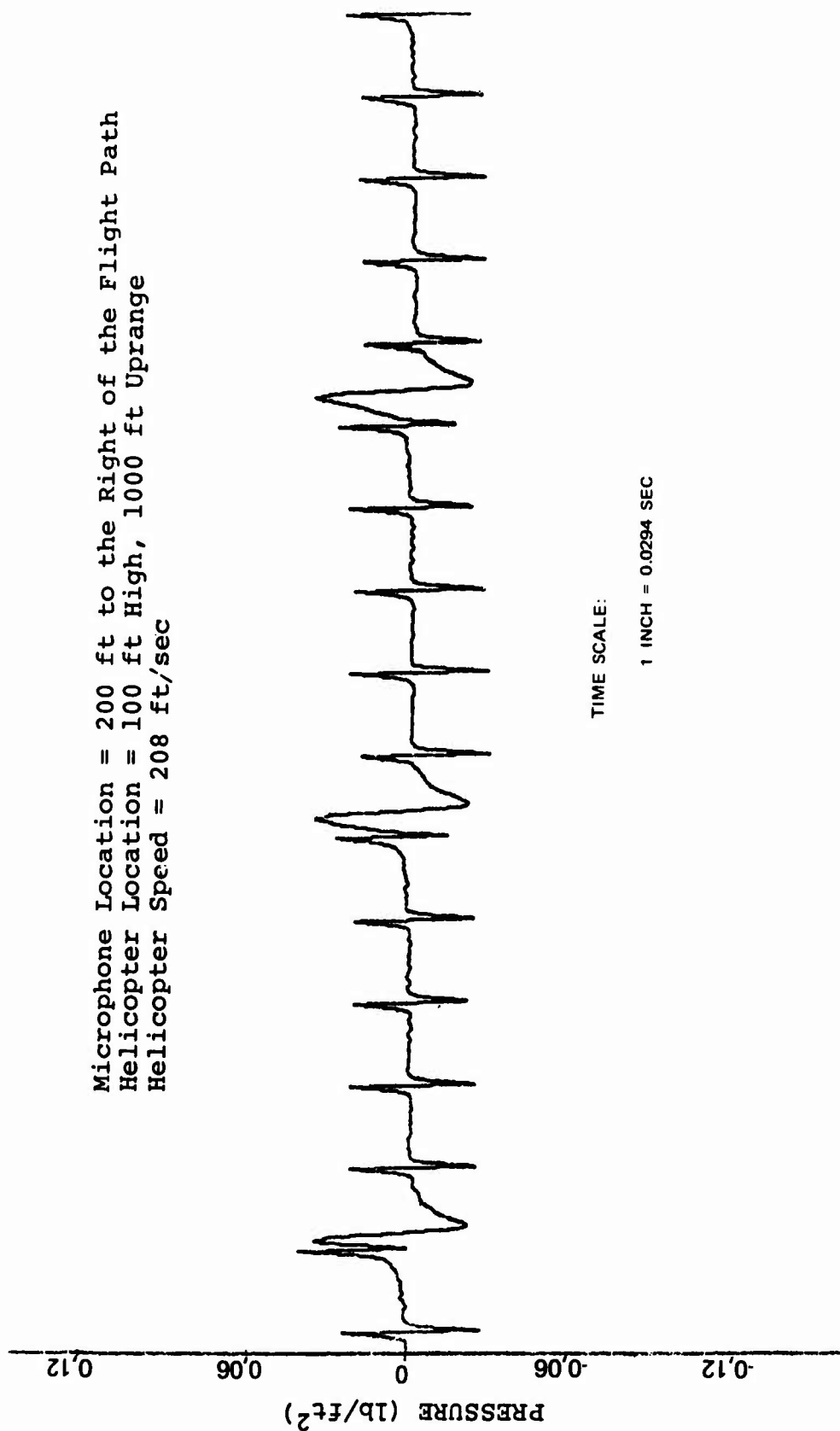
Figure 9. Pressure Time History of Predicted Noise Generated From a UH-1B in Level Flight.

31

Microphone Location: 200 ft to the Right of the Flight Path
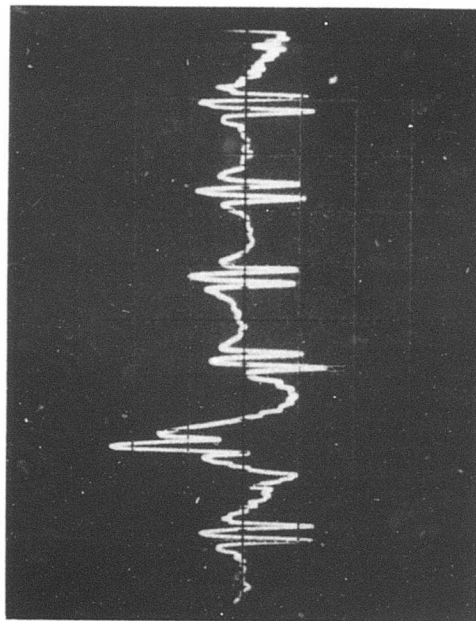Helicopter Location: 100 ft High, 700 ft Uprange
Helicopter Speed: 208 ft/sec

Experimental Pressure Time History
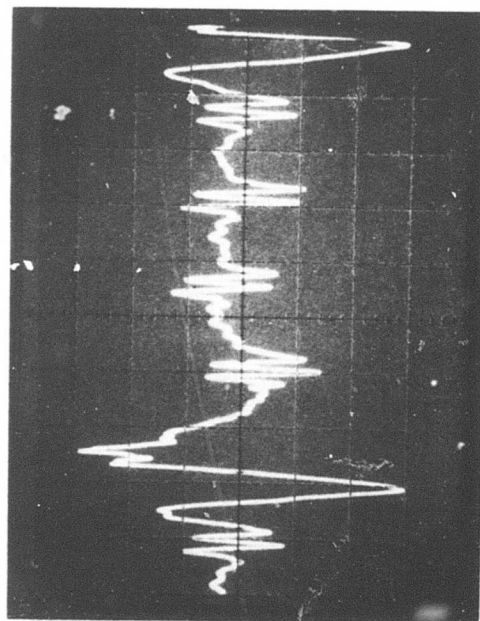Vertical Scale: 1 cm is 0.08 lb/ft^2
Horizontal Scale: 1 cm is 0.01 sec

Predicted Pressure Time History
Vertical Scale: 1 cm is 0.06 lb/ft^2
Horizontal Scale: 1 cm is 0.01 sec

Figure 10. Pressure Time Histories of Noise From a UH-1B in Level Flight.

Microphone Location: 200 ft to the Right of the Flight Path
Helicopter Location: 100 ft High, 500 ft Uprange
Helicopter Speed: 208 ft/sec

Experimental Pressure Time History
Vertical Scale: 1 cm is 0.08 lb/ft^2
Horizontal Scale: 1 cm is 0.01 sec

Predicted Pressure Time History
Vertical Scale: 1 cm is 0.06 lb/ft^2
Horizontal Scale: 1 cm is 0.01 sec

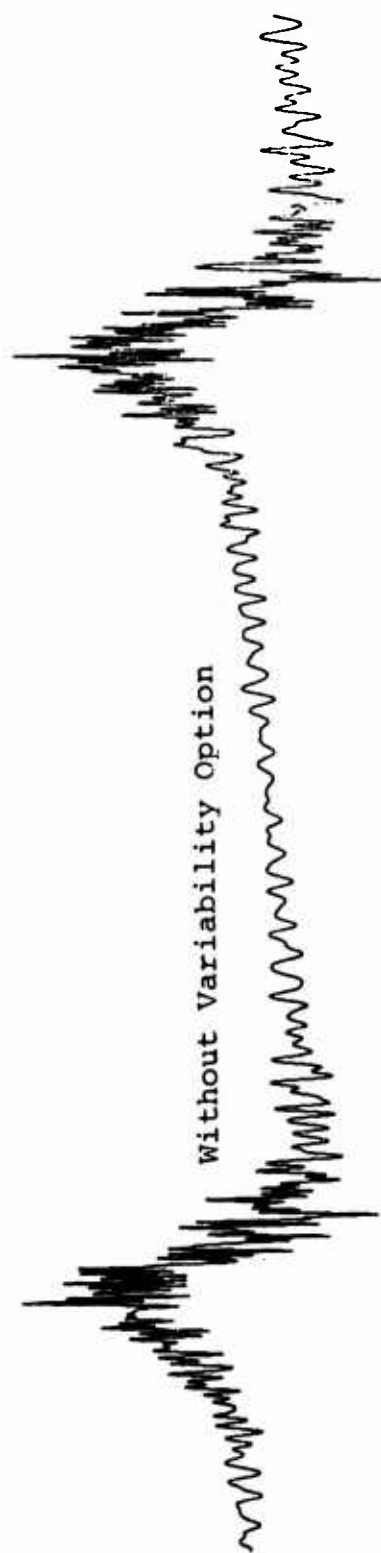Figure 11.   Pressure Time Histories of Noise From a UH-1B in Level Flight.

Microphone Location: 200 ft to the Right of the Flight Path
Helicopter Location: 100 ft High, 350 ft Uprange
Helicopter Speed: 208 ft/sec

Experimental Pressure Time History
Vertical Scale: 1 cm is 0.08 lb/ft^2
Horizontal Scale: 1 cm is 0.01 sec

Predicted Pressure Time History
Vertical Scale: 1 cm is 0.06 lb/ft^2
Horizontal Scale: 1 cm is 0.01 sec

Figure 12. Pressure Time Histories of Noise From a UH-1B in Level Flight.

34

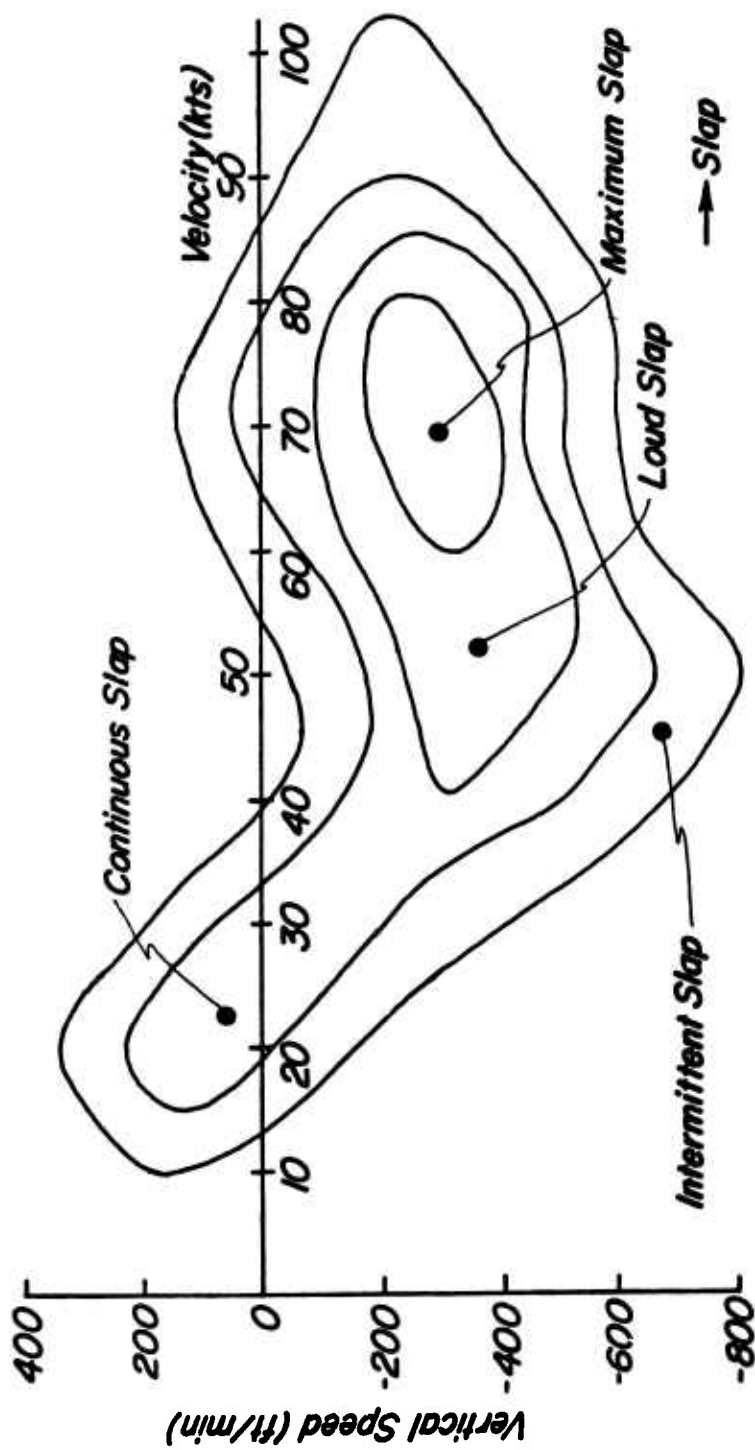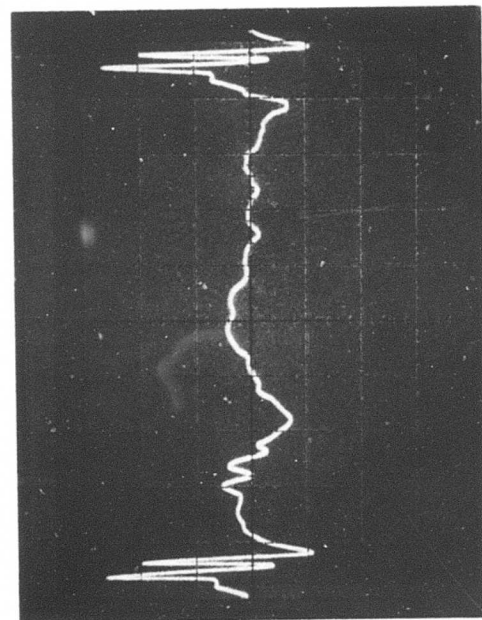Figure 13. Pressure Time Histories of Predicted Noise From a UH-1D Main Rotor in Hover.

35

Figure 14. Flight Conditions Associated With Main Rotor Blade Slap for 10,000 - Lb Class Helicopters (From Reference 6).

Microphone Location: 450 ft to the Right of the Flight Path
Helicopter Location: 1000 ft High, 1600 ft Uprange
Helicopter Speed: 42 ft/sec

Predicted Noise with Blade Vortex Inter-
action
Vertical Scale: 1 cm is 0.0016 lb/ft^2
Horizontal Scale: 1 cm is 0.01 sec
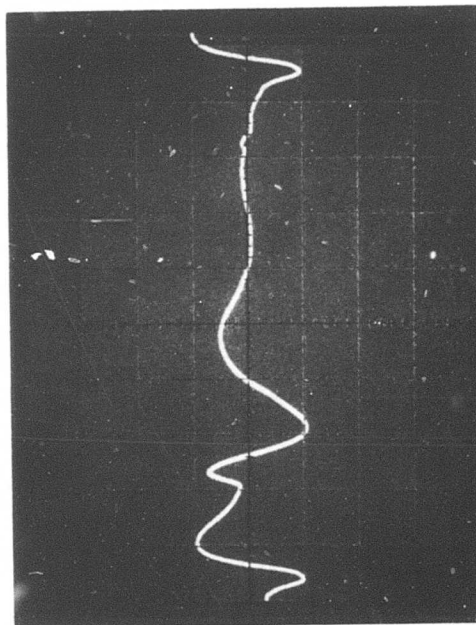
Predicted Noise Without Blade Vortex
Interaction
Vertical Scale: 1 cm is 0.0017 lb/ft^2
Horizontal Scale: 1 cm is 0.01 sec

Figure 15. Pressure Time History of Predicted Rotational Noise Generated From
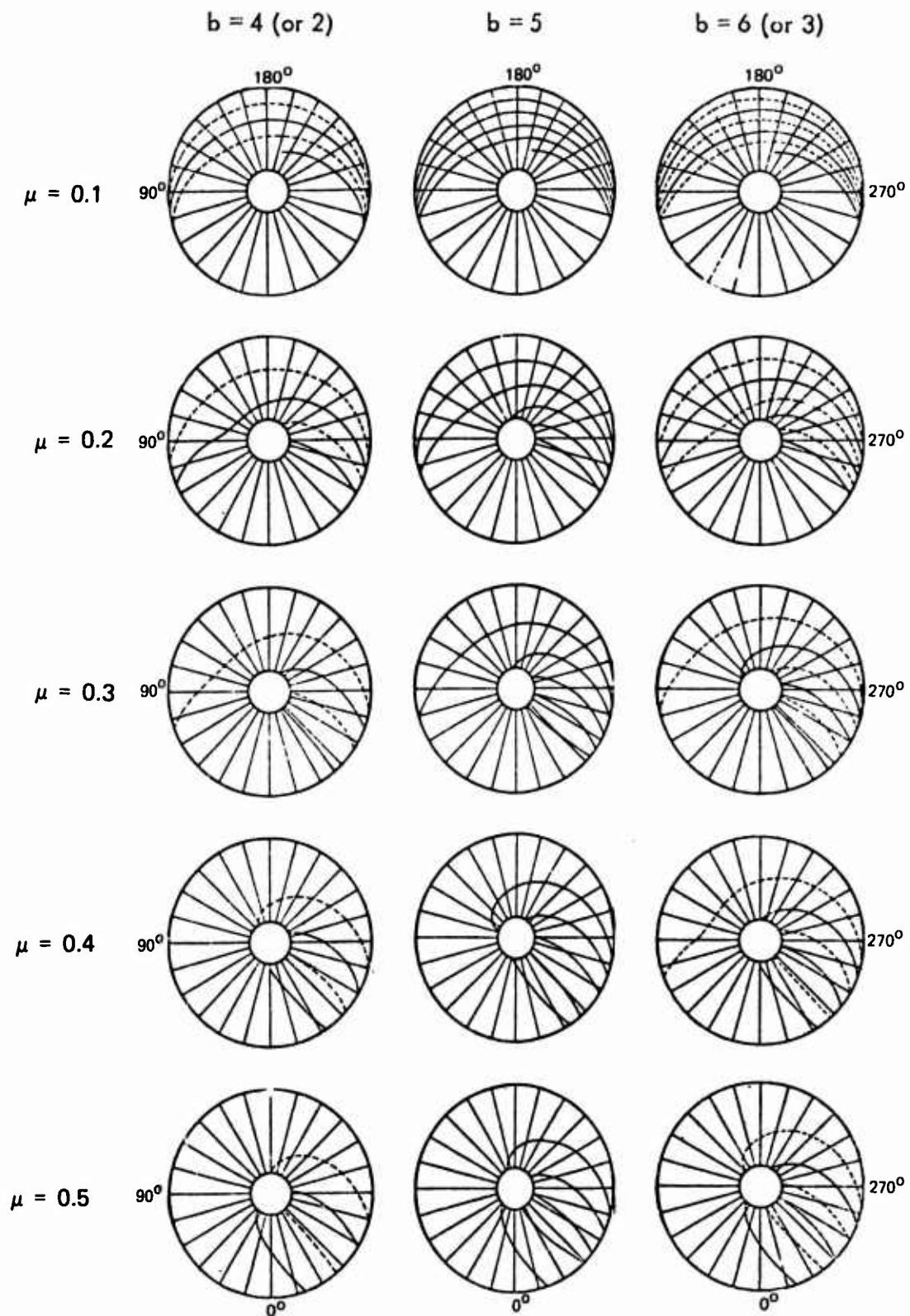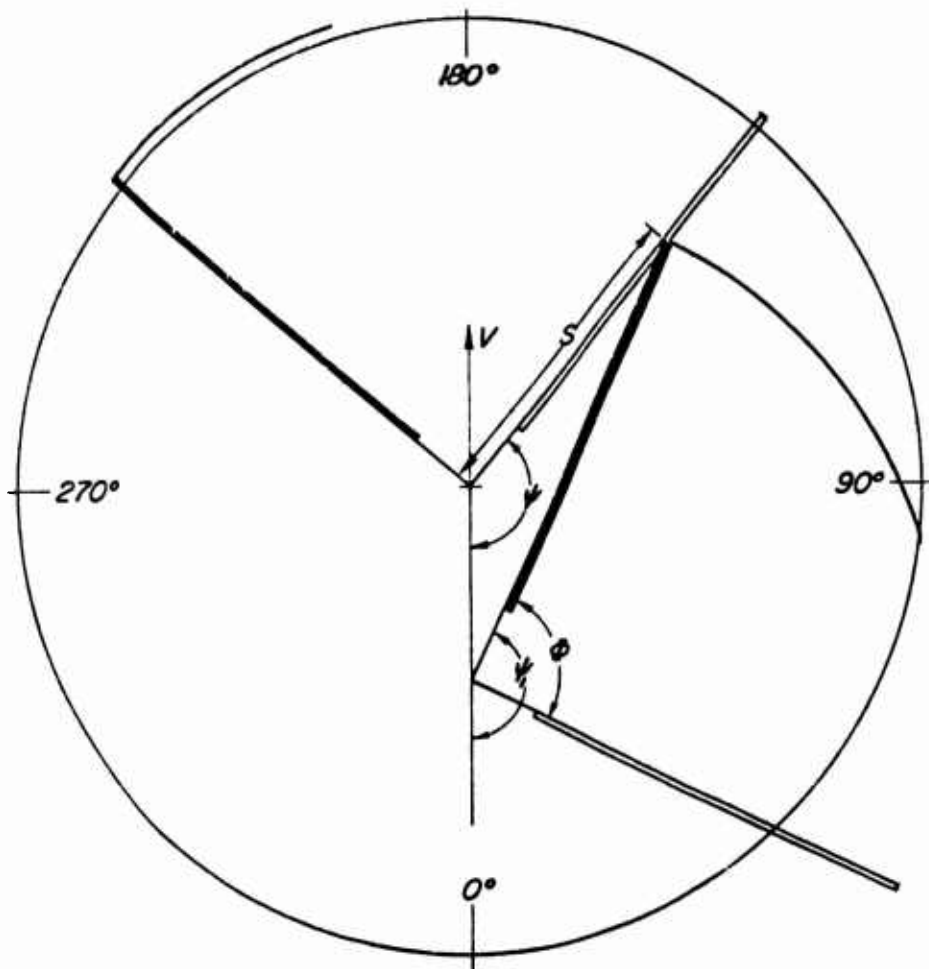a UH-1D Main Rotor in Level Flight.

37

Figure 16. Loci of Blade/Vertex Intersection Points as a Function of Advance Ratio and Number of Blades (From Reference 2).

38

Black Blade: Vortex Shedding Blade
White Blade: Vortex Intersecting Blade

Figure 17. Geometry of a Single Rotor Blade Vortex
Interaction.

39

LIST OF SYMBOLS

c	speed of sound (ft/sec)
$\underline{d}$	distance of microphone from source along the ground (ft)
f_a	frequencies at which the ground-reflected signal is in phase with the direct signal (Hz)
f_c	frequencies at which the ground-reflected signal is $180°$ out of phase with the direct signal (Hz)
GRC	ground reflection coefficient
$\underline{h}$	altitude of noise source (ft)
$\underline{\ell}$	microphone height (ft)
$\underline{\ell}_{max}$	20 ft
M	velocity of the blade station divided by the speed of sound
n	non-negative integer
P_{osc}	oscillatory lift per square foot at the blade station (lb/ft^2)
S_t	Strouhal number
th	blade section thickness as seen by the flow (ft)
u	flow velocity (ft/sec)
α	angle of attack
ω	vortex shedding frequency (Hz)

6691-74